JACS
JOURNAL OF THE AMERICAN CHEMICAL SOCIETY

Article

pubs.acs.org/JACS

Mechanistic Studies of Two-Dimensional Covalent Organic Frameworks Rapidly Polymerized from Initially Homogenous Conditions

Brian J. Smith and William R. Dichtel*

Department of Chemistry and Chemical Biology, Baker Laboratory, Cornell University, Ithaca, New York 14853-1301, United States

Supporting Information

ABSTRACT: Covalent organic frameworks (COFs) are periodic two- and three-dimensional (2D and 3D) polymer networks with high surface areas, low densities, and designed structures. Despite intense interest in framework materials, the nucleation and growth processes of COFs, and even of more established metal−organic frameworks (MOFs), are poorly understood. The kinetics of COF growth under varied reaction conditions provides mechanistic insight needed to improve their crystallinity and rationally synthesize new materials. Such kinetic measurements are unprecedented and difficult to perform on typical heterogeneous COF reaction mixtures. Here we synthesize 2D boronate ester-linked COF-5 under conditions in which the monomers are fully soluble. These homogeneous growth conditions provide equal or better material quality compared to any previous report and enable the first rigorous studies of the early stages of COF growth. COF-5 forms within minutes, and the precipitation rate is readily quantified from optical turbidity measurements. COF-5 formation follows an Arrhenius temperature dependence between 60−90 °C with an activation energy of 22−27 kcal/mol. The measured rate law includes a second order in both boronic acid and catechol moieties, and inverse second order in MeOH concentration. A competitive monofunctional catechol slows COF-5 formation but does not redissolve already precipitated COF, indicating both dynamic covalent bond formation and irreversible precipitation. Finally, stoichiometric H_2O provides a 4-fold increase in crystallite domain areas, representing the first rational link between reaction conditions and material quality.

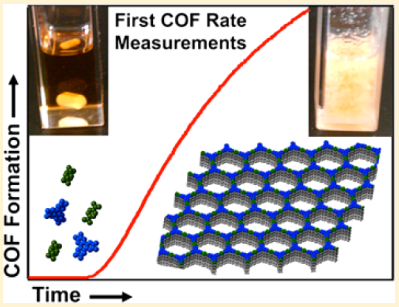

1. INTRODUCTION

Covalent organic frameworks (COFs)[1−9] are an emerging class of porous, periodic two- and three-dimensional (2D and 3D) polymers that have attracted interest for diverse applications, including chemical separations, gas storage,[10] catalysis,[11−13] and optoelectronic[14−18] and charge storage[19] devices. COFs are distinct from molecular compounds and linear polymers because they organize monomers predictably into networks with well-defined pores and high internal surface areas. Their structural precision rivals that of designed supramolecular assemblies, yet they are robust, covalently linked materials. Despite these desirable features, COFs remain far from fulfilling their potential because they are typically isolated as microcrystalline powders of limited utility. The poorly understood simultaneous polymerization and crystallization processes stall efforts to improve COF crystallinity, access surface areas that approach theoretical values, control crystal and thin-film morphologies, and identify new COF linkage chemistries.

Our poor understanding of COF growth means that synthesizing a new framework, even one that uses established chemical linkages, involves empirical guesswork rather than rational experimental design.[20] Discovery is reduced to an exhaustive search of solvent combinations and concentrations, temperature, reaction time, and even atmosphere identity, pressure, and reaction vessel volume, with failed experiments providing no insight for improvement. When COF thin films are desired,[21] optimal growth conditions often differ from those that provide polycrystalline powders, and thin-film thickness control is undemonstrated. In contrast to the more established class of metal−organic frameworks[22−24] (MOFs), no single-crystal structure of a 2D COF has been reported to date, and only one 3D COF, an azodioxy-linked 3D network,[25] has been characterized by single-crystal X-ray diffraction.[26]

Understanding how COFs nucleate and grow will address these challenges and inform the development of new frameworks. For example, it has been assumed that COF polymerizations must feature reversible bond formation to provide crystalline products, yet recent polycrystalline frameworks linked by β-ketoenamines,[19,27,28] hydrazones,[29] and azines[7,30,31] suggest that rapid covalent bond exchange might not be a strict requirement. Furthermore, nucleation processes are unstudied in COFs, are poorly understood for MOFs, and are still actively studied for many traditional crystallizations.[20,32−34] However, characterizing COF growth processes faces a major hurdle: in most reported syntheses[2] the monomers are only partially soluble under the reaction conditions (Figure 1). The COF product also precipitates from the reaction mixture, causing the solution to remain heterogeneous. Indeed, partial monomer dissolution has been

Received: April 16, 2014
Published: May 22, 2014

   dx.doi.org/10.1021/ja5037868 | J. Am. Chem. Soc. 2014, 136, 8783−8789

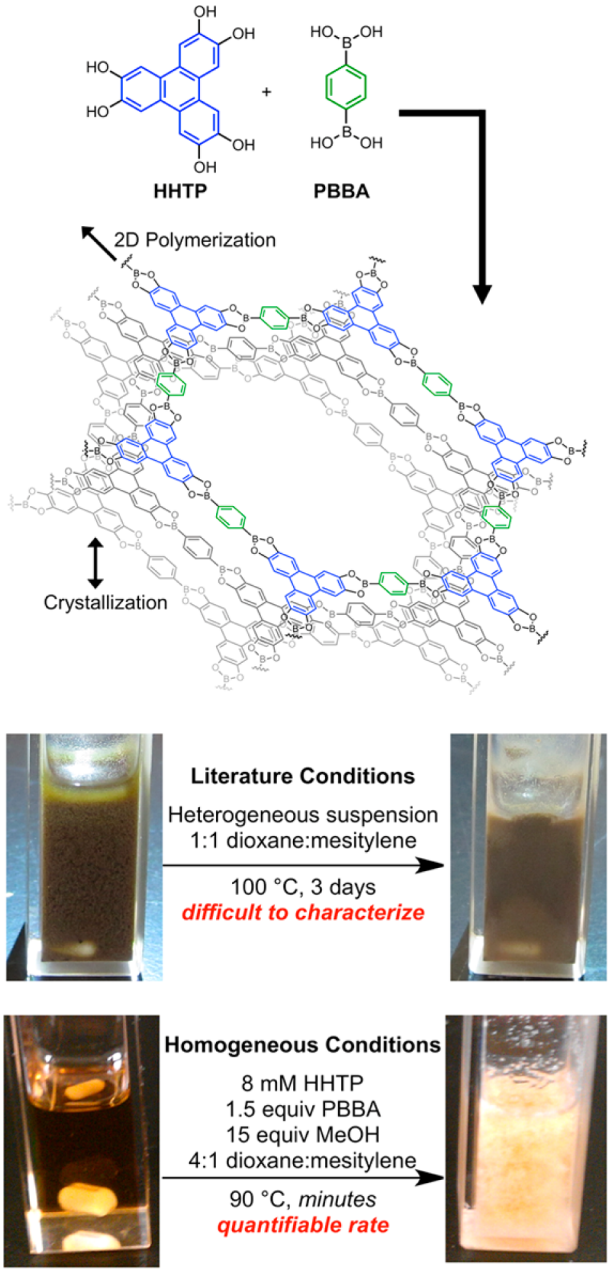

Figure 1. A comparison of heterogeneous and homogeneous growth conditions for COF-5.

suggested to contribute to COF crystallization,[35] despite the tendency of remaining insoluble monomers and oligomers to clog the pores of the isolated materials. This heterogeneity precludes the use of most *in situ* spectroscopic characterization techniques to gain insight into COF polymerization and crystallization processes.

Here we synthesize the prototypical hexagonal 2D framework, COF-5, under initially homogeneous conditions, allowing us to measure the rate of COF-5 formation for the first time and to characterize its sensitivity to varied reaction conditions. Polymerization in the presence of a soluble monofunctional catechol competitor slows the rate of COF formation and confirms that the growth features at least one irreversible step. Finally, we can rationally increase and control the average crystallite size by adding H_2O. We anticipate that these findings will inspire further rigorous studies of COF nucleation and polymerization that will further improve crystallinity and facilitate the discovery of new frameworks.

2. RESULTS

2.1. Homogeneous Synthesis and Turbidity Characterization. Synthesizing COFs from initially homogeneous solutions is a prerequisite for studying and rationally improving their growth conditions. Previously reported syntheses provide the 2D hexagonal network COF-5 as a microcrystalline powder, which exhibits a surface area of ca. 1600 m^2/g following extended solvent washing to remove residual molecular contaminants.[1] The 2,3,6,7,10,11-hexahydroxytriphenylene (HHTP) and 1,4-phenylenebis(boronic acid) (PBBA) monomers are only partially soluble under literature conditions (1:1 dioxane/mesitylene), causing the COF to coprecipitate with the starting material. We screened solvent and additive combinations that fully dissolve the reactants and found that 4:1 dioxane/mesitylene with small amounts of MeOH (15 equiv relative to HHTP) form homogeneous solutions. Upon heating to 90 °C, precipitate begins to form within minutes. Filtration after 20 h provided 75% isolated yield of the COF-5 product, whose FTIR and powder X-ray diffraction (PXRD) matched previous reports. The isolated COF exhibited a BET surface area (N_2 adsorption) of ca. 2000 m^2/g without postsynthetic extractions, which exceeds the original report[1] and is comparable to the highest values obtained using sonication or microwave activation.[35,36] Overall, these homogeneous growth conditions provide COF-5 of equal or better quality relative to previous reports and enable the mechanistic studies described below.

Homogeneous growth conditions provide an unprecedented opportunity to measure the rate of COF formation and determine its sensitivity to experimental parameters. The reaction mixture clouds as COF-5 precipitates, such that the stirred solution's turbidity provides a means to measure the observed rate of COF formation. Turbidity measurements have been employed to study nanoparticle interactions,[37] polymer micelle formation,[38] protein aggregation,[39] mineral precipitation,[40] and bacterial growth. The rate of COF powder formation is directly proportional to the *in situ* optical turbidity of the reaction mixture (Figure 2) at 1310 nm. At this wavelength, absorption from solvent vibrational modes and trace oxidized HHTP side products is minimal (see Supporting Information Figure S2), such that changes in transmission

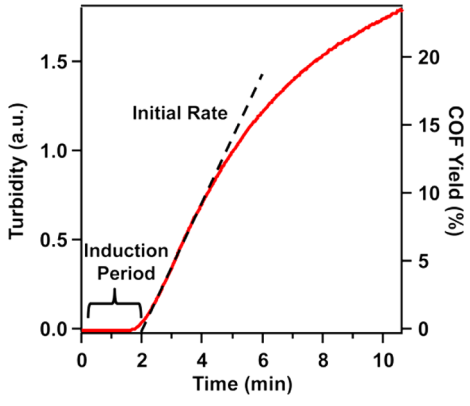

Figure 2. Turbidity measurement of COF-5 formation as a function of time (8 mM HHTP, 1.5 equiv of PBBA, 15 equiv of MeOH, 4:1 dioxane/mesitylene, 90 °C).

dx.doi.org/10.1021/ja5037868 | J. Am. Chem. Soc. 2014, 136, 8783−8789

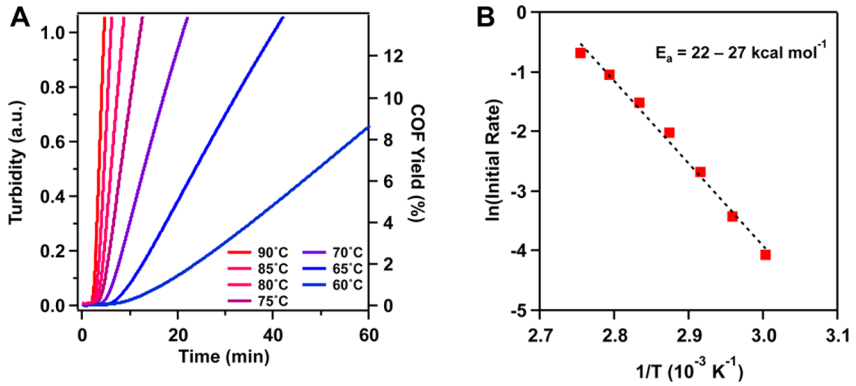

Figure 3. (A) COF-5 formation over time at various temperatures. (B) Pseudo-Arrhenius plot of the initial rate of COF-5 formation.

correspond to light scattering associated with COF-5 precipitation. COF-5 precipitation begins after a 2 min induction period and proceeds at a constant rate for several minutes, after which it begins to slow. Although the COF formation rate is very sensitive to the solution composition (see below), the rates are reproducible (see Supporting Information Figure S3). The precipitate was confirmed to be crystalline COF-5 by PXRD analysis of the solids filtered from the solutions at various reaction times. Notably, the precipitate collected after only 5 min corresponds to 17% yield and exhibited PXRD peaks at 3.5, 6.0, 9.1, and 26.5 deg (2θ, Cu kα) that are associated with the COF-5 lattice (see Supporting Information Figure S4). Precipitate collected at 5 min, 10 min, 20 min, 1 h, 8 h, and 20 h, respectively, also exhibited identical PXRD patterns associated with COF-5 (see Supporting Information Figure S10), and no evidence of cocrystallized monomers or other impurities was observed. The solution turbidity was calibrated by suspending independently prepared COF-5 powder in reaction solvent. Turbidity is linearly dependent on the suspension concentration up to 1 mg/mL, corresponding to 27% yield under these conditions (see Supporting Information Figure S5). The spectroscopically measured yield of COF-5 at 5 min is 15%, which is consistent with the gravimetrically measured yield of the isolated solid, further validating the turbidity calibration. These combined observations indicate that the solid that first precipitates from the reaction mixture is crystalline COF-5, and the initial changes in turbidity, once appropriately calibrated, represent a direct measure of the rate of COF formation.

2.2. Kinetic Analysis. Monitoring the COF growth rate under various homogeneous reaction conditions provides new insight into their bond-forming and crystallization processes. COF-5 formation is an activated process; longer induction periods and slower formation rates are observed at lower reaction temperatures (Figure 3). Solid confirmed to be crystalline COF-5 by PXRD was observed within the first hour at temperatures as low as 60 °C. The initial rate of COF-5 formation exhibits well-behaved temperature dependence, affording a nearly linear pseudo-Arrhenius plot derived from the initial rates. A slight curvature to the temperature dependence broadens the range of activation energies (22–27 kcal/mol). This value is comparable to those calculated for the formation of a Cu-paddlewheel MOFs (17–27 kcal/mol).[41,42] These observations demonstrate that COF-5 crystallizes readily over at least a 30 °C temperature range and that temperature control might improve 2D COF synthesis by controlling the formation rate.

The effect of the HHTP, PBBA, and MeOH concentrations on COF formation was determined by the method of initial rates. The independent reaction orders of the HHTP and PBBA monomers cannot be determined under pseudo-first order conditions because crystalline COF-5 is formed only near the ideal 3:2 molar ratio of PBBA/HHTP. Using a large excess of one monomer impacts the equilibrium esterification and provides amorphous polymer samples. Instead, we measured the COF-5 formation rate at different initial concentrations, always maintaining $[\text{catechol}]_0$ = $[\text{boronic acid}]_0$ (i.e., 3:2 $[\text{PBBA}]_0/[\text{HHTP}]_0$). Serial dilution from the initial concentrations (8 mM HHTP, 1.5 equiv PBBA, 15 equiv MeOH) yields an overall second order rate dependence (see Supporting Information Figure S6). The dependence on MeOH was determined independently. Although a minimum amount of MeOH (10–15 equiv relative to HHTP) is necessary to fully dissolve the monomers, excess MeOH slows COF-5 formation. For example, <1% precipitation is observed within 1 h when 100 or more equivalents of MeOH are employed. COF-5 formation displays an inverse second order dependence on MeOH concentration (see Supporting Information Figure S7). This dependence, in addition to the overall rate order, yields a general expression for the rate of COF-5 growth as a function of initial monomer and MeOH concentrations (Figure 4). Empirically, a second order dependence on both boronic acid and catechol species is observed, under the condition of

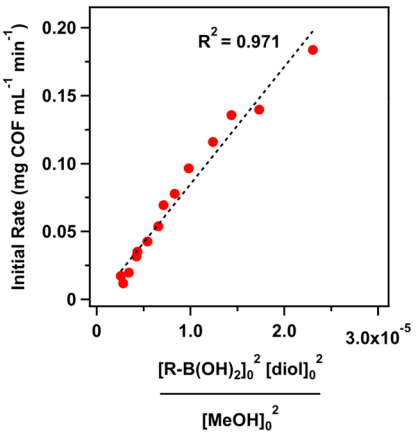

Figure 4. Initial rate of COF-5 formation as a second order function of $[\text{diol}]_0$ and $[\text{R-B(OH)}_2]_0$ and an inverse second order function of MeOH concentration. The expression is only valid when $[\text{diol}]_0$ = $[\text{R-B(OH)}_2]_0$.

dx.doi.org/10.1021/ja5037868 | J. Am. Chem. Soc. 2014, 136, 8783–8789

$[\text{catechol}]_0 = [\text{boronic acid}]_0$. This relationship provides a means of rationally predicting and targeting a particular COF growth rate, in contrast to the ill-defined, unnecessarily long waiting periods (72 h for COF-5) reported for these materials grown under heterogeneous conditions.

We obtained further mechanistic insight into COF formation by adding a competing monofunctional catechol species. Truncated monomers have been used to control the crystal morphology of MOFs[43] and to internally functionalize 3D COFs.[44−46] In contrast, their effect on 2D COF formation has not been reported. Here, 4-*tert*-butylcatechol (TCAT) is used as a truncated equivalent of HHTP, which reversibly forms soluble catechol boronate esters with PBBA that are non-productive for the COF polymerization (Figure 5A). As expected, COF-5 forms more slowly in the presence of TCAT—the induction period increases, and the initial rate of precipitation decreases. Overall, an inverse first order dependence in [TCAT] is observed (see Supporting Information Figure S8). Compared to MeOH, the rate of COF-5 formation is more sensitive to the presence of TCAT; whereas COF-5 precipitation occurs within minutes in the presence of 20 equiv of MeOH relative to HHTP, 20 equiv of TCAT results in no appreciable solid formation within 1 h. Most notably, although TCAT slows the rate of COF-5 formation significantly, it does not impact the isolated yields that were obtained. For example, the isolated yield of COF-5 formed in the presence of 6.0 equiv of TCAT, polymerized for 5 days, is 70%, as compared to 77% under similar conditions in the absence of TCAT. Furthermore, TCAT is not incorporated into the isolated COF-5 product, as determined by hydrolyzing COF-5 isolated from reaction mixtures containing 6.0, 9.0, or 12 equiv of TCAT. ^{1}H NMR spectroscopic analysis of the hydrolysis products revealed no TCAT (Figure 6), which stands in stark contrast to 3D boroxine-linked COFs, in which truncated monomers have been shown to comprise as much as 34 mol % of the crystalline network, COF-102.[46] Overall, the decreasing rate in the presence of TCAT indicates that TCAT serves as a competitor to HHTP during the polymerization of COF-5, and boronate ester formation occurs reversibly. However, the high isolated yields of COF-5 and the lack of TCAT incorporation in the final product indicate that there is an irreversible process downstream of covalent bond formation that serves as a driving force for COF formation.

Adding TCAT after the onset of COF precipitation sheds further light on the interplay between dynamic covalent bond formation and irreversible processes that occur under the reaction conditions. The introduction of 6.0 equiv of TCAT relative to HHTP to the reaction mixture after the onset of turbidity, providing a 2:1 ratio of nonproductive to productive catechol moieties, immediately decreases the rate of precipitation (Figure 5B). The new rate is similar to that observed when 6.0 equiv of TCAT are present at t = 0. The instantaneous change in the rate of COF-5 formation upon TCAT addition indicates that the bond-forming processes are highly dynamic under these conditions. We performed a similar experiment with 30 equiv of TCAT, corresponding to a 10-fold excess of nonproductive catechols relative to those present in HHTP (Figure 5C). No COF-5 precipitate forms over extended times when this amount of TCAT is present initially. This finding is consistent with the rate data on the influence of TCAT on the induction period, which predicts an induction period of days (see Supporting Information Figure S8C). Likewise, COF-5 formation stops immediately when 30 equiv

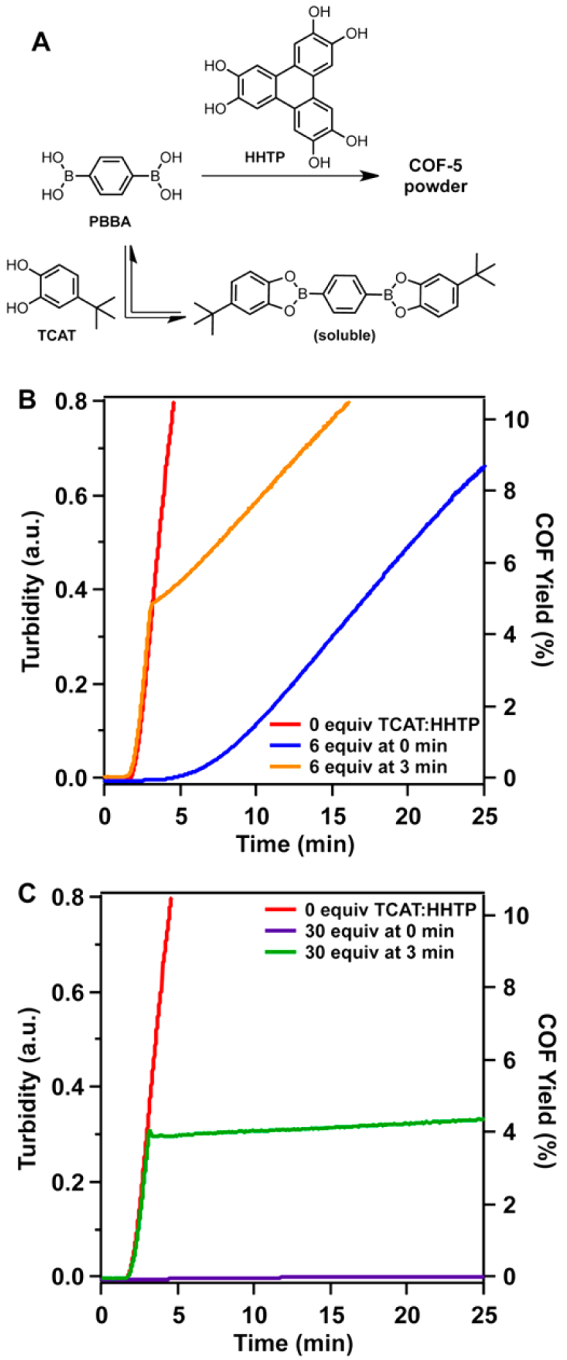

Figure 5. (A) TCAT as a competitor for boronate ester formation. (B) Addition of 6 equiv of competitor TCAT at either 0 or 3 min. (C) Addition of 30 equiv of competitor TCAT at either 0 or 3 min, demonstrating irreversibility of COF-5 precipitation.

of TCAT are introduced, as evident from the lack of further increase in turbidity. However, the late addition of even a large excess of TCAT does not *decrease* the turbidity. That TCAT fails to redissolve COF-5 suggests that the COF forms irreversibly. We propose that 2D COF formation relies on a kinetically irreversible step, after which the product is chemically inaccessible, rendering boronate ester formation irreversible as well. We hypothesize that irreversible COF precipitation limits the crystallite sizes for 2D COFs.

Surmising that larger crystallites might be obtained by maintaining reversible bond formation, we examined the effect

dx.doi.org/10.1021/ja5037868 | J. Am. Chem. Soc. 2014, 136, 8783−8789

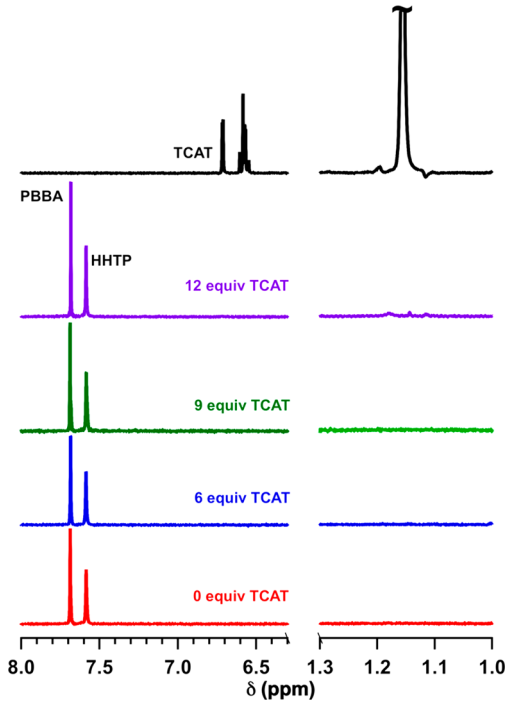

Figure 6. Partial ^{1}H NMR spectra [400 MHz, 298 K, DMSO-d_6/D_2O (99:1 v/v)] of TCAT and hydrolyzed COF-5 synthesized in the presence of various amounts of TCAT (0–12 equiv). In all hydrolyzed COF-5 samples, no evidence of the *t*-butyl moiety or aromatic resonances of TCAT is observed.

of reversible hydrolysis of boronate ester species by added H_2O. Improved long-range order upon exposure of H_2O vapor was reported for boroxine monolayers prepared under UHV conditions.[47] Added H_2O inhibits COF formation, displaying an inverse first order dependence (see Supporting Information Figure S9). Added H_2O also systematically increases the average in-plane crystalline domain size (Figure 6, Supporting Information Figure S11), as judged by applying the Scherrer equation to the ⟨100⟩ peak (3.5 deg 2θ, Cu kα). Fifteen equivalents of added H_2O (relative to HHTP) provide an average in-plane domain diameter of 40 nm, which is approximately double that obtained in the absence of added H_2O, corresponding to a 4-fold increase in the average area of the covalently linked crystalline domains. In contrast, samples grown in the presence of TCAT exhibit only a limited increase in crystalline domain size, with a maximum observed diameter of ca. 30 nm. More than 20 equiv of added H_2O caused little to no COF-5 to precipitate after several days, indicating that there is an upper practical limit to H_2O addition as a means to obtain larger COF-5 crystals. Scanning electron micrographs of COF-5 powders grown in the presence of 0–18 equiv of H_2O (Supporting Information Figures S12–S17) display similar few-micrometer size particles with only minor textural differences, indicating that these amounts of added H_2O do not induce major changes in the final polycrystalline aggregates. These experiments represent the first systematic control over crystallite domain size of a COF and implicate rational control over COF morphology.

3. DISCUSSION

Homogenous conditions for COF-5 growth have enabled the first rate measurements of COF formation. Furthermore, controlling the reaction temperature, concentration, and

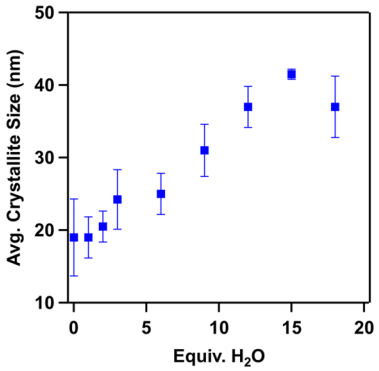

Figure 7. In-plane average crystallite size as a function of equivalents of water added relative to HHTP. Each value is the average of at least two runs.

additive concentrations provides new insight into COF polymerizations and crystallizations, leading to a model for COF-5 formation shown in Figure 8. The early stages of COF-5 growth presumably involve monomers condensing into soluble oligomers, similar to a step-growth polymerization. Subsequent nucleation affords COF crystallites of unknown structure and size, which might be as small as a single macrocyclic hexagon. The crystallites grow by further bond formation and stacking processes until they achieve the average sizes and thicknesses ascertained by X-ray diffraction. These small crystallites also aggregate and precipitate as a polycrystalline, high surface area powder, which forms within minutes in the absence of excess TCAT, MeOH, or H_2O. The speed of this process and early observed crystallinity contrasts with amorphous aggregate crystallizations previously observed for zeolites,[48] in which an initially amorphous precipitate crystallizes over an extended time period.

These studies demonstrate that 2D boronate ester COF-5 formation includes both reversible bond forming processes and at least one irreversible step. The monofunctional catechol competitor TCAT lengthens the induction period and inhibits precipitation, even when added *during* the polymerization. However, TCAT is not incorporated into COF-5, even when used in excess, and it does not limit the isolable yields of COF-5. These combined observations indicate that dynamic boronate ester exchange occurs among soluble monomers and oligomers and presumably at the growing crystal fronts prior to precipitation. In contrast, the final polycrystalline COF precipitates irreversibly, resisting dissolution by a large excess of TCAT. Two independent observations are consistent with this claim: First, we are unaware of any demonstration of Ostwald ripening of COF-5 and other COF crystallites over extended reaction times; second, 3D COFs crystallize in the presence of large excesses (>30 equiv) of competing monofunctional monomers.[46] Collectively, these results strongly suggest that both 2D and 3D COF syntheses proceed through a system of reversible equilibria, which is capped by at least one irreversible step that drives the formation of the polycrystalline product.

This study bases its conclusions on measurements of the rate of COF-5 precipitation as micrometer-sized polycrystalline particles. Though much new insight into COF formation has been gained, our understanding of the nucleation, polymerization, and crystal growth prior to aggregation remains incomplete. For example, laminar crystals might arise from the formation of larger 2D polymers of increasing size and decreasing solubility, which ultimately stack into layered

dx.doi.org/10.1021/ja5037868 | J. Am. Chem. Soc. 2014, 136, 8783–8789

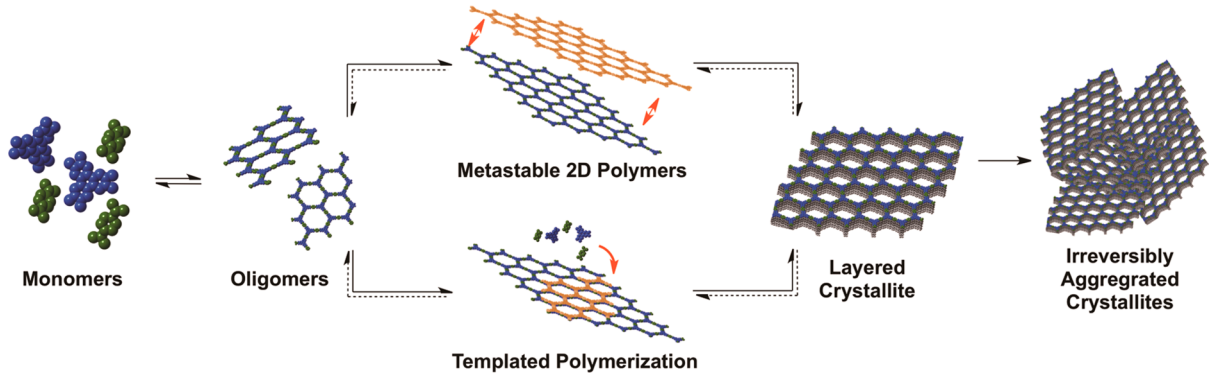

Figure 8. Proposed models of boronate ester COF-5 growth.

structures. Alternatively, smaller oligomers may stack upon larger 2D polymers, leading to a templated polymerization through monomer addition. We favor this latter scenario based on the virtually complete exclusion of TCAT from COF-5 grown in the presence of a large excess of this competitor. The observed rate dependence (second order in both boronic acid and catechol) might be explained by a rate-determining step involving interlayer boronate ester stacking. In this model, the observed inverse second order dependence on [MeOH] might correspond to the formation of dispersed MeOH-boronate complexes, which must expel MeOH to crystallize. We will continue to clarify the key rate determining processes of COF-5 formation by further characterizing the earliest stages of fully homogeneous oligomer growth and will generalize these techniques to other 2D and 3D COFs.

The quality of COF materials must improve for these frameworks to fully realize their potential. Methods to access increased crystallite sizes (ideally single crystals) and surface areas that approach theoretical values must be prioritized. This study achieves rational but modest increases in crystallite size by including small amounts of H_2O, which decreases the rate by imparting reversible and partial hydrolysis during synthesis. Catechol competitors, by contrast, did not show the same effect. These findings demonstrate that rational manipulation of framework growth conditions can provide improved morphological control. We anticipate that additional means of inhibiting aggregation might lead to improved reversibility and, ultimately, a broader array of accessible COF materials.

4. CONCLUSION

The boronate ester-linked 2D framework COF-5 is readily synthesized from fully homogeneous conditions on time scales of minutes, which enabled the first rate measurements of its formation. This rate, quantified by simple turbidity measurements, is reproducible and exhibits an Arrhenius temperature dependence. The kinetic sensitivity to concentration and additives provides mechanistic insight into how these materials form. COF-5 growth features both dynamic bond forming processes, as well as at least one irreversible step associated with the precipitation of the nanocrystalline powder. We have demonstrated systematic control over the size of crystalline domain by adding excess H_2O. These techniques are readily applicable to other COF networks and will facilitate future studies of COF nucleation processes, the rational improvement of COF crystallization conditions, and the discovery of new frameworks.

■ ASSOCIATED CONTENT

Supporting Information

Experimental procedures, characterization data, and rate order calculations. This material is available free of charge via the Internet at http://pubs.acs.org.

■ AUTHOR INFORMATION

Corresponding Author

E-mail: wdichtel@cornell.edu.

Notes

The authors declare no competing financial interest.

■ ACKNOWLEDGMENTS

This research was supported by the NSF CAREER award (CHE-1056657), a Cottrell Scholar Award from the Research Corporation for Scientific Advancement, the Alfred P. Sloan Foundation, and a Camille Dreyfus Teacher-Scholar Award from the Camille and Henry Dreyfus Foundation. We also made use of the Cornell Center for Materials Research Shared Facilities, which are supported through the NSF MRSEC program (DMR-1120296).

■ REFERENCES

(1) Côté, A. P.; Benin, A. I.; Ockwig, N. W.; O'Keeffe, M.; Matzger, A. J.; Yaghi, O. M. *Science* **2005**, *310*, 1166.
(2) Tilford, R. W.; Gemmill, W. R.; zur Loye, H.-C.; Lavigne, J. J. *Chem. Mater.* **2006**, *18*, 5296.
(3) Tilford, R. W.; Mugavero, S. J.; Pellechia, P. J.; Lavigne, J. J. *Adv. Mater.* **2008**, *20*, 2741.
(4) Spitler, E. L.; Dichtel, W. R. *Nat. Chem.* **2010**, *2*, 672.
(5) Feng, X.; Ding, X.; Jiang, D. *Chem. Soc. Rev.* **2012**, *41*, 6010.
(6) Ding, S.-Y.; Wang, W. *Chem. Soc. Rev.* **2012**, *42*, 548.
(7) Jackson, K. T.; Reich, T. E.; El-Kaderi, H. M. *Chem. Commun.* **2012**, *48*, 8823.
(8) Colson, J. W.; Dichtel, W. R. *Nat. Chem.* **2013**, *5*, 453.
(9) Kandambeth, S.; Shinde, D. B.; Panda, M. K.; Lukose, B.; Heine, T.; Banerjee, R. *Angew. Chem., Int. Ed.* **2013**, *52*, 13052.
(10) Doonan, C. J.; Tranchemontagne, D. J.; Glover, T. G.; Hunt, J. R.; Yaghi, O. M. *Nat. Chem.* **2010**, *2*, 235.
(11) Ding, S.-Y.; Gao, J.; Wang, Q.; Zhang, Y.; Song, W.-G.; Su, C.-Y.; Wang, W. *J. Am. Chem. Soc.* **2011**, *133*, 19816.
(12) Xu, H.; Chen, X.; Gao, J.; Lin, J.; Addicoat, M.; Irle, S.; Jiang, D. *Chem. Commun.* **2014**, *50*, 1292.
(13) Fang, Q.; Gu, S.; Zheng, J.; Zhuang, Z.; Qiu, S.; Yan, Y. *Angew. Chem., Int. Ed.* **2014**, *53*, 2878.
(14) Spitler, E. L.; Colson, J. W.; Uribe-Romo, F. J.; Woll, A. R.; Giovino, M. R.; Saldivar, A.; Dichtel, W. R. *Angew. Chem., Int. Ed.* **2012**, *51*, 2623.

(15) Bertrand, G. H. V.; Michaelis, V. K.; Ong, T.-C.; Griffin, R. G.; Dincă, M. *Proc. Natl. Acad. Sci. U. S. A.* **2013**, *110*, 4923.
(16) Dogru, M.; Handloser, M.; Auras, F.; Kunz, T.; Medina, D.; Hartschuh, A.; Knochel, P.; Bein, T. *Angew. Chem., Int. Ed.* **2013**, *52*, 2920.
(17) Wan, S.; Guo, J.; Kim, J.; Ihee, H.; Jiang, D. *Angew. Chem., Int. Ed.* **2008**, *47*, 8826.
(18) Wan, S.; Guo, J.; Kim, J.; Ihee, H.; Jiang, D. *Angew. Chem., Int. Ed.* **2009**, *48*, 5439.
(19) DeBlase, C. R.; Silberstein, K. E.; Truong, T.-T.; Abruña, H. D.; Dichtel, W. R. *J. Am. Chem. Soc.* **2013**, *135*, 16821.
(20) Wang, F.; Richards, V. N.; Shields, S. P.; Buhro, W. E. *Chem. Mater.* **2014**, *26*, 5.
(21) Colson, J. W.; Woll, A. R.; Mukherjee, A.; Levendorf, M. P.; Spitler, E. L.; Shields, V. B.; Spencer, M. G.; Park, J.; Dichtel, W. R. *Science* **2011**, *332*, 228.
(22) Robson, R. *J. Chem. Soc., Dalton Trans.* **2000**, 3735.
(23) Yaghi, O. M.; O'Keeffe, M.; Ockwig, N. W.; Chae, H. K.; Eddaoudi, M.; Kim, J. *Nature* **2003**, *423*, 705.
(24) Furukawa, H.; Cordova, K. E.; O'Keeffe, M.; Yaghi, O. M. *Science* **2013**, *341*, 1230444.
(25) Beaudoin, D.; Maris, T.; Wuest, J. D. *Nat. Chem.* **2013**, *5*, 830.
(26) Recently, the structure of micron-sized crystallites of a 3D imine-linked COF was characterized by electron diffraction. The COF's crystallite size and aggregated morphology was typical of previously reported materials. See Zhang, Y.-B.; Su, J.; Furukawa, H.; Yun, Y.; Gándara, F.; Duong, A.; Zou, X.; Yaghi, O. M. *J. Am. Chem. Soc.* **2013**, *135*, 16336.
(27) Kandambeth, S.; Mallick, A.; Lukose, B.; Mane, M. V.; Heine, T.; Banerjee, R. *J. Am. Chem. Soc.* **2012**, *134*, 19524.
(28) Biswal, B. P.; Chandra, S.; Kandambeth, S.; Lukose, B.; Heine, T.; Banerjee, R. *J. Am. Chem. Soc.* **2013**, *135*, 5328.
(29) Uribe-Romo, F. J.; Doonan, C. J.; Furukawa, H.; Oisaki, K.; Yaghi, O. M. *J. Am. Chem. Soc.* **2011**, *133*, 11478.
(30) Ren, S.; Bojdys, M. J.; Dawson, R.; Laybourn, A.; Khimyak, Y. Z.; Adams, D. J.; Cooper, A. I. *Adv. Mater.* **2012**, *24*, 2357.
(31) Dalapati, S.; Jin, S.; Gao, J.; Xu, Y.; Nagai, A.; Jiang, D. *J. Am. Chem. Soc.* **2013**, *135*, 17310.
(32) Davey, R. J.; Schroeder, S. L. M.; ter Horst, J. H. *Angew. Chem., Int. Ed.* **2013**, *52*, 2166.
(33) Vekilov, P. G. *Nanoscale* **2010**, *2*, 2346.
(34) Desiraju, G. R. *Nat. Mater.* **2002**, *1*, 77.
(35) Yang, S.-T.; Kim, J.; Cho, H.-Y.; Kim, S.; Ahn, W.-S. *RSC Adv.* **2012**, *2*, 10179.
(36) Campbell, N. L.; Clowes, R.; Ritchie, L. K.; Cooper, A. I. *Chem. Mater.* **2009**, *21*, 204.
(37) Dutta, N.; Egorov, S.; Green, D. *Langmuir* **2013**, *29*, 9991.
(38) Bhargava, P.; Tu, Y.; Zheng, J. X.; Xiong, H.; Quirk, R. P.; Cheng, S. Z. D. *J. Am. Chem. Soc.* **2007**, *129*, 1113.
(39) Borgia, M. B.; Nickson, A. A.; Clarke, J.; Hounslow, M. J. *J. Am. Chem. Soc.* **2013**, *135*, 6456.
(40) Dorozhkina, E. I.; Dorozhkin, S. V. *Colloids Surf. Physicochem. Eng. Asp.* **2002**, *203*, 237.
(41) Goesten, M. G.; Stavitski, E.; Juan-Alcañiz, J.; Martiñez-Joaristi, A.; Petukhov, A. V.; Kapteijn, F.; Gascon, J. *Catal. Today* **2013**, *205*, 120.
(42) Millange, F.; Osta, R. E.; Medina, M. E.; Walton, R. I. *CrystEngComm* **2010**, *13*, 103.
(43) Tsuruoka, T.; Furukawa, S.; Takashima, Y.; Yoshida, K.; Isoda, S.; Kitagawa, S. *Angew. Chem., Int. Ed.* **2009**, *48*, 4739.
(44) Bunck, D. N.; Dichtel, W. R. *Chem.—Eur. J.* **2013**, *19*, 818.
(45) Bunck, D. N.; Dichtel, W. R. *Angew. Chem., Int. Ed.* **2012**, *51*, 1885.
(46) Brucks, S. D.; Bunck, D. N.; Dichtel, W. R. *Polymer* **2014**, *55*, 330.
(47) Guan, C.-Z.; Wang, D.; Wan, L.-J. *Chem. Commun.* **2012**, *48*, 2943.
(48) Mintova, S.; Olson, N. H.; Valtchev, V.; Bein, T. *Science* **1999**, *283*, 958.